animals

MDPI

Article

Investigating the Effects of the *Taraxacum kok-saghyz* Rodin Polysaccharide on Intestinal Immune Function in Lambs Based on the "Gut Microbiota–Metabolites" Axis

Xiaohui Zhang [1,2,3], Saifuding Abula [2,3], Yan Zhang [1], Abudukeyoumu Abudurezike [1], Qiang Gao [1], Ayjamal Keram [1], Jiamin Cao [1], Lisi Tang [1], Tuhanguli Tuoheti [1], Lin Xu [1] and Zulikeyan Manafu [1,2,*]

[1] Crop Research Institute of Xinjiang Uygur Autonomous Region Academy of Agricultural Sciences/National Central Asian Characteristic Crop Germplasm Resources Medium-Term Bank, Urumqi 830091, China; zxhxxdsh@163.com (X.Z.)
[2] College of Veterinary Medicine, Xinjiang Agricultural University, Urumqi 830052, China
[3] Xinjiang Key Laboratory of New Drug Study and Creation for Herbivorous Animal (XJ-KLNDSCHA), Xinjiang Agricultural University, Urumqi 830052, China
* Correspondence: zulikeyan@163.com

Simple Summary

Plant polysaccharides may help regulate intestinal health in livestock, but their effects can vary depending on the plant part from which they are obtained. In this study, 21 lambs were divided into three groups and received either no polysaccharide treatment, *Taraxacum kok-saghyz* Rodin leaf polysaccharide (TKP-L), or *Taraxacum kok-saghyz* Rodin root polysaccharide (TKP-R) for 28 days. Both polysaccharides were associated with changes in intestinal immune-related markers. TKP-L was associated with higher intestinal PIgR gene expression and a stronger IgA immunofluorescence signal, whereas TKP-R was associated with a stronger ZO-1 signal, a marker related to intestinal barrier integrity. Fecal microbiota analysis revealed differences in microbial community composition and the enrichment of specific bacterial groups. Exploratory metabolomic analysis also suggested differences in jejunal metabolites between treatments; however, the overall metabolomic profiles did not differ significantly among the groups, and the predicted molecular pathways and microbiota–metabolite relationships require further validation. These findings provide preliminary evidence that leaf- and root-derived polysaccharides may have different associations with intestinal immune-related responses in lambs.

Abstract

Objective: To investigate the differential regulatory effects of *Taraxacum kok-saghyz* Rodin leaf polysaccharide (TKP-L) and *Taraxacum kok-saghyz* Rodin root polysaccharide (TKP-R) on intestinal immune function in lambs, and to explore the potential association between the gut microbiota and jejunal metabolites. Methods: After a 7-day adaptation period, twenty-one two-month-old male lambs were randomly divided into three groups ($n = 7$ per group): control (CK), TKP-L, and TKP-R. The feeding trial lasted 28 days. TKP-L and TKP-R were administered orally by gavage at 400 mg/kg body weight per day, while the CK group received no additional treatment. At the end of the trial, all lambs were euthanized, and samples were collected for tissue and omics analyses ($n = 7$ per group). Exploratory network pharmacology prediction based on human databases was used to generate candidate targets and pathways, which guided the selection of subsequent in vivo parameters. qPCR was used to detect the mRNA expression of PIgR, TNF-α, and IL-6 in the duodenum and jejunum. HE staining and immunofluorescence were used to evaluate liver and intestinal morphology and the expression of ZO-1 and IgA. 16S rRNA sequencing was used to analyze

Check for updates

Academic Editors: Bingyu Shen, Chenxu Zhao and Hongming Lv

Received: 3 September 2026
Revised: 10 November 2026
Accepted: 16 November 2026
Published: 18 November 2026

Copyright: © 2026 by the authors. Licensee MDPI, Basel, Switzerland. This article is an open access article distributed under the terms and conditions of the Creative Commons Attribution (CC BY) license.

the fecal microbiota. Untargeted metabolomics was used to analyze jejunal metabolites. Correlations between fecal microbiota and jejunal metabolites were then analyzed. Results: Exploratory network pharmacology prediction suggested 47 and 27 candidate intersection targets for TKP-L and TKP-R, respectively, which were predicted to be enriched in neuroactive ligand–receptor interaction and calcium signaling pathways. Neither TKP-L nor TKP-R induced statistically significant changes in duodenal pIgR, TNF-α, or IL-6 mRNA expression or jejunal pIgR mRNA expression compared with the CK group. Although numerical variations were observed, these differences were not statistically significant. Jejunal IL-6 expression differed significantly between the TKP-L and TKP-R groups, whereas neither treatment group differed significantly from the CK group. Immunofluorescence showed that TKP-R was associated with a higher ZO-1 signal, whereas TKP-L showed a stronger IgA immunofluorescence signal. However, secreted sIgA and barrier function were not directly measured. 16S rRNA analysis showed that polysaccharide treatment did not significantly change α diversity but was associated with the enrichment of specific bacteria (TKP-L: *Oscillospiraceae*; TKP-R: *Ruminococcaceae*). Untargeted metabolomics showed that TKP-L was mainly associated with changes in inflammation-related lipid mediators (PGI2 and Lipoxin B4), while TKP-R was mainly associated with changes in anti-inflammatory polyunsaturated fatty acids (EPA and α-linolenic acid). Correlation analysis revealed that the abundance of *Prevotella* was positively correlated with immunomodulatory metabolites such as Curine and LPI-18-1. Conclusions: TKP-L and TKP-R were associated with differential changes in selected intestinal immune markers, fecal microbiota composition, and jejunal metabolites in lambs. TKP-L was associated with higher PIgR mRNA and IgA immunofluorescence signals, whereas TKP-R was associated with a higher ZO-1 signal. However, the predicted targets and pathways were not validated in lamb tissues. In addition, secreted sIgA, intestinal barrier function, growth performance, nutrient utilization, and the efficacy of TKP as a feed additive were not directly evaluated. These findings provide preliminary evidence and require further investigation. Exploratory untargeted metabolomics suggested candidate abundance differences in selected jejunal metabolite features, whereas global metabolite profiles did not differ significantly among groups (PERMANOVA, $p = 0.2258$). The metabolite-level patterns and microbiota–metabolite associations warrant further validation.

Keywords: *Taraxacum kok-saghyz* Rodin polysaccharide; lamb; intestinal immunity; gut microbiota; metabolomics; network pharmacology

1. Introduction

With the rapid and intensive development of animal husbandry, young animals face increasing risks of pathogen exposure during the critical stages before and after weaning, which seriously threatens the health of lambs and the economic benefits of breeding. The lamb stage is an important window for the growth and development of ruminants. At this time, the immune system is not mature and the digestive function is not perfect. Under intensive production conditions, the combination of multiple factors such as environmental pathogens, poor maternal condition, and early nutritional deficiency often leads to the development of the immune system being inhibited and disease resistance decreased, and then a variety of intestinal and systemic diseases are induced [1]. Although traditional means such as antibiotics, chemical drugs, and vaccines are widely used in animal health assurance, the side effects caused by them, such as microbial resistance, drug residues in animal products, and immunosuppression, have attracted increasing attention, and there is an urgent need to find safe and effective alternative strategies to antibiotics [2,3].

Plant-derived polysaccharides are becoming one of the hot spots in antibiotic substitution research because of their stable structure, good biocompatibility, and multi-target regulation ability [4,5]. However, their efficacy as antibiotic alternatives in lambs has not yet been established and requires further investigation. Unlike traditional therapeutic drugs, plant polysaccharides are difficult for host digestive enzymes to decompose, but they can be used as fermentation substrates for intestinal flora, selectively promoting the proliferation of beneficial symbiotic bacteria such as *Prevotella*. Studies have shown that *Prevotella* can promote the generation of IL-10-producing regulatory T cells (Treg) and activate the Th17 pathway by stimulating mucosal pattern recognition receptors [6,7]. A variety of metabolites (such as short-chain fatty acids, PGI2, phenyl sulfate, Curine, etc.) produced by intestinal microbial fermentation of polysaccharides also play a key role in immune regulation. As immunomodulators from natural sources, plant polysaccharides can affect host immune response and intestinal microecological balance through a variety of mechanisms. However, whether TKP-L and TKP-R act through similar mechanisms in lambs remains unknown. We hypothesized that TKP-L and TKP-R may differentially regulate intestinal immune function by modulating the gut microbiota and jejunal metabolites. Studies have confirmed that *Helianthus tuberosus* polysaccharide can increase the abundance of fiber-degrading bacteria such as *Prevotella* and *Succiniclasticum* in the rumen, significantly increase the concentration of propionic acid, and reduce the level of ammonia nitrogen in the rumen [8]. Together, these studies reveal that plant polysaccharides play a comprehensive and fine regulatory role in regulating the structure of intestinal flora, promoting the production of beneficial metabolites, and enhancing immune function through the "microbiota–metabolism–host" interaction network, which has good prospects for development and application.

Taraxacum kok-saghyz Rodin, also known as Russian dandelion, is another important member of the genus *Taraxacum*. It is a perennial herb rich in natural inulin fructan, and has important economic value as an alternative source of natural rubber in Xinjiang of our country and Central Asia [9]. In addition to rubber, the remaining biomass of rubber plants is also rich in bioactive components such as polysaccharides, flavonoids, and triterpenoids. However, knowledge on the biological activity of *Taraxacum kok-saghyz* Rodin polysaccharide (TKP) has been almost non-existent for a long time, and initial progress has been made only recently. Liang confirmed in a mouse mastitis model that polysaccharides derived from rubber leaf can reduce mammary gland inflammation, enhance the expression of tight junction proteins in the intestine and mammary gland, prevent intestinal bacterial translocation, and reconstruct microbial homeostasis in the intestine and milk through the "gut–mammary axis" [10]. Aersilan further found in sheep lambs that TKP-L could enhance the expression of the mucin gene in intestinal mucosa, enrich bacteria such as *Prevotellaceae_UCG-001*, *Butyrivibrio*, and *Paraprevotella*, and increase the level of argininosuccinic acid through the amino acid metabolism pathway [11]. Correlation analysis showed that the abundance of argininosuccinate was significantly positively correlated with the amount of *Prevotellaceae_UCG-001*, suggesting that TKP-L may promote growth and immune function of lambs through the regulation of argininosuccinate metabolism mediated by *Prevotella*.

Although initial progress has been made in the application of polysaccharides from rubber plants in ruminants, there are still many key problems to be explored. In this study, we took *Taraxacum kok-saghyz* Rodin polysaccharide as the research object, and predicted the targets and related signaling pathways of *Taraxacum kok-saghyz* Rodin polysaccharide in the growth immunity of lambs using network pharmacological analysis. By measuring the levels of intestinal growth and immune-related genes, analyzing the histomorphological parameters of the gastrointestinal tract, and analyzing the expression of tight junction proteins, we revealed the immunomodulatory effect of *Taraxacum kok-saghyz* Rodin polysaccharides.

16S rRNA gene sequencing and untargeted metabolomics technology were used to analyze the composition and succession of intestinal microbial community and the changes of metabolite profiles in lambs under the action of *Taraxacum kok-saghyz* Rodin polysaccharide, and to construct a "microbiota–metabolite" interaction network. The purpose of this study was to systematically reveal the regulatory mechanism of *Taraxacum kok-saghyz* Rodin polysaccharide as a new green feed additive in the growth and immune protection of lambs, and to provide part of the basis for the development of *Taraxacum kok-saghyz* Rodin polysaccharide as a green feed additive in the healthy breeding of ruminants.

2. Materials and Methods

2.1. Preparation of Rubber Polysaccharides

Taraxacum kok-saghyz leaf polysaccharide (TKP-L) and *T. kok-saghyz* root polysaccharide (TKP-R) were extracted and prepared in the laboratory. The crude polysaccharide was obtained by water extraction and alcohol precipitation. The protein was deproteinized via the Sevag method, and the small molecular substances were removed by dialysis and freeze-dried before use. The crude polysaccharide content of TKP-L and TKP-R was 39.44 ± 1.98% and 48.32 ± 2.42%, respectively, and the polysaccharide yield was 5.19 ± 0.77% and 9.61 ± 0.76%, respectively [11]. Monosaccharide composition was determined by high-performance liquid chromatography–front column derivatization (PMP-HPLC). The settings for the ThermoU3000 liquid chromatography system, with chromatographic column Agilent ZORBAX EclipseXDB-C18 (4.6 × 250 mm, 5 μm) (Thermo Fisher Scientific Inc., Waltham, MA, USA) and acetonitrile in the mobile phase, were as follows: the volume ratio of acetonitrile to phosphate buffer was 17:83, the flow rate was 0.8 mL/min, the column temperature was 30 °C, the detection wavelength was 250 nm, and the injection volume was 10 μL. The monosaccharide composition of TKP-L was 74.51% Galacturonic Acid, 9.38% Arabinose, 7.02% Galactose, 5.34% Rhamnose, 1.21% Xylose, 1.05% Glucuronic Acid, 0.91% Fucose, 0.58% Glucose; TKP-R consisted of 59.19% Galacturonic Acid, 23.34% Arabinose, 11.81% Galactose, 2.99% Rhamnose, and 2.68% Glucose.

2.2. Screening of Candidate Active Ingredients

The monosaccharide constituent units of TKP-L and TKP-R were used as the objects of analysis. The monosaccharides in TKP-L and TKP-R were listed, including glucose, glucuronic acid, galactose, arabinose, fucose, xylose, rhamnose, and galacturonic acid, from the PubChem database (https://pubchem.ncbi.nlm.nih.gov) to obtain the monosaccharide Canonical SMILES format and 3 d structure (SDF format).

2.3. Prediction of Potential Targets of Taraxacum kok-saghyz Rodin Polysaccharides

The monosaccharide components contained in TKP-L and TKP-R were separately predicted for targets and combined to obtain candidate target sets for the two polysaccharides. SwissTargetPrediction Prediction: the SMILES string of each monosaccharide was entered separately, "*Homo sapiens*" was selected for species, and the Probability threshold (Probability) was set to >0.1 to retain the predicted target protein. The UniProt ID and Gene Symbol of each target were recorded to obtain the target set of rubber leaf polysaccharide (Targets_TKP-L) and root polysaccharide (Targets_TKP-R).

2.4. Screening of Targets Related to Growth and Immunity in Lambs

Since the existing disease databases are mainly based on human data, this study used a strategy that combined human orthologous genes with a literature supplement to obtain target sets related to the growth performance and immune function of lambs. GeneCards database search: "growth performance", "body weight gain", "average daily

gain", "immune response", "immunomodulation", "inflammation", "lamb", "growth", and "sheep immunity" were used as keywords to search in the GeneCards database. The search results of each keyword were sorted by Relevance Score, and genes were selected for merging. OMIM database search: the items referring to Mendelian diseases related to growth retardation, growth hormone deficiency, and immunodeficiency were searched, and their related genes were extracted. Finally, the "lamb growth immunity" disease target set (Targets_Disease) was obtained. Because no sheep-specific target database was available, human databases were used for exploratory target prediction. Where possible, human genes were mapped to sheep orthologs. This approach is limited by species differences and does not represent direct evidence of intact TKP targets in lambs.

2.5. Acquisition of Drug–Disease Intersection Targets

The intersection of Targets_TKP-L, TKP-R, and Targets_Disease was used to obtain the potential targets of *Taraxacum kok-saghyz* Rodin leaf polysaccharide (Candidates_TKP-L) and the potential targets of *Taraxacum kok-saghyz* Rodin root polysaccharide (Candidates_TKP-R). At the same time, the intersection targets shared by the two methods and their unique targets were calculated, and a Venn diagram was drawn.

2.6. PPI Network Construction and Core Target Screening

Candidates_TKP-L and Candidates_TKP-R were imported into the STRING 12.0 database, and the species was set to "*Homo sapiens*" to hide the unconnected nodes in the network. The TSV-format interaction relationship file was downloaded. The interaction file exported by STRING was imported into Cytoscape 3.10.4 software. The "NetworkAnalyzer" tool was used to calculate the following topological parameters of each node: Degree Centrality (DC), Betweenness Centrality (BC), Closeness Centrality (Closeness Centrality, CC), and Eigenvector Centrality (EC). The DC value of all nodes was more than 2 times the median DC value of all nodes as the screening condition, and the hub targets were screened. The core targets of TKP-L and TKP-R were obtained and compared.

2.7. GO Functional Enrichment and KEGG Pathway Analysis

The gene lists of Candidates_TKP-L and Candidates_TKP-R were submitted to the DAVID 6.8 online platform, and the species was selected as "*Homo sapiens*". "Biological Process" (BP) and "KEGG Pathway" under "Gene Ontology" were selected for enrichment analysis. The threshold was set as Count ≥ 2, $p < 0.05$. Significantly enriched entries were retained. The top 20 GO BP entries with the smallest p value (or FDR) and all KEGG pathways in each analysis were screened, and the online tool was used to draw enrichment bubble maps. The similarities and differences in pathway enrichment between TKP-L and TKP-R were compared.

2.8. Construction of "Component–Target–Pathway" Network

Three types of nodes were constructed: component nodes (monosaccharides contained in TKP-L/TKP-R); Target nodes (Candidates_TKP-L or Candidates_TKP-R); Pathway nodes (the top 10 significant pathways selected from KEGG enrichment results). Edge connection rules: the component–target edge was derived from prediction results such as SwissTargetPrediction (corresponding relationship with prediction probability > 0.1); target–pathway was derived from the official pathway–gene mapping relationship of the KEGG database (if the target belonged to the pathway, it was connected). The node file and side file were imported in Cytoscape, and different shapes were set according to the node type (component: diamond, target: circle, path: V). The "yFiles Organic" layout algorithm was used to arrange the network. The size of a node was mapped to a Degree value (larger nodes are larger),

and the thickness of an edge was mapped to a Combined score (for target–target edges) or confidence (for component–target edges). The "NetworkAnalyzer" of Cytoscape was used to calculate the global network parameters (average node degree, network diameter, clustering coefficient, etc.) and identify the key modules in the network. The top 10 nodes were selected as the network core nodes by MCC algorithm in the CytoHubba plugin.

2.9. Experimental Animals

Twenty-one two-month-old male lambs with similar body weight and good health were selected. Upon arrival, all lambs were acclimatized for 7 days before the start of the feeding trial. During the adaptation period, the lambs received the same basal diet and had free access to water, without TKP supplementation or other medication. Body weight and feed intake were not measured during this period, and no specific health measurements were taken; however, no clinical abnormalities were observed. After adaptation, the lambs were stratified according to body weight and randomly assigned to three groups ($n = 7$ per group): control (CK), TKP-L, and TKP-R. The feeding trial lasted 28 days. All 21 lambs were housed together in a single pen under the same feeding, management, and environmental conditions. The animals were individually identified using distinct markings to distinguish the three experimental groups (CK, TKP-L, and TKP-R; $n = 7$ per group). Each lamb was considered an individual experimental unit for the experimental measurements and statistical analyses, and each lamb provided animal-level biological samples for the corresponding analyses, yielding seven animal-level observations per treatment group. All animal experiments were performed in the Veterinary Hospital of Xinjiang Agricultural University. The Experimental Animal Welfare Ethics Committee of Xinjiang Agricultural University approved this trial (approval number: 2025020) to ensure compliance with all relevant ethical regulations for animal experimentation and research. All animal experiments were conducted in accordance with the ARRIVE guidelines (https://arriveguidelines.org). Enclosures and the barn were cleaned and disinfected every 5 days. Temperature, relative humidity, and photoperiod were not continuously monitored. All groups were maintained under identical feeding, management, and environmental conditions. The control group received no additional treatment. The TKP-L and TKP-R groups received 400 mg/kg body weight per day of the corresponding polysaccharide by oral gavage, and TKP-L and TKP-R were administered individually. All lambs had free access to water and were fed ad libitum. Although all lambs shared the same housing environment, potential interactions among animals and their effects on the intestinal microbiota could not be completely excluded. On the 28th day, all 7 lambs in each group were euthanized. Before euthanasia, they were electrocuted to render them unconscious, and their lives were terminated by bleeding through the jugular vein. Death was confirmed by the absence of a heartbeat and corneal reflex. Samples of the liver, duodenum, jejunum, ileum, and feces were collected for the analyses described in Sections 2.10–2.13. All samples were collected at the same time point at the end of the experiment.

2.10. mRNA Expression of Immunoglobulin A and Immune-Related Genes in Each Intestinal Segment of Lambs

Two cm of each midduodenum and jejunum was collected as described in Section 2.9, and intestinal contents were gently washed with precooled sterile PBS, flash frozen in liquid nitrogen, and stored at −80 °C. Total RNA was extracted by the TRIzol method and operated according to the kit instructions. cDNA was synthesized using a reverse transcription kit and stored at −20 °C. RT-qPCR was used to detect the relative expression levels of PIgR, Tnf-α, and IL-6 mRNA in the duodenum and jejunum. The reaction conditions were as follows: predenaturation at 95 °C for 30 s, with [GAPDH] as an internal control; 40 cycles

of 95 °C for 5 s, 60 °C for 30 s. This was followed by melting curve analysis. The $2^{-\Delta\Delta Ct}$ method was used to calculate the relative expression, and the CK group was used as the calibration group. Primer sequences are shown in Table 1.

Table 1. Primers list.

Gene	Sense Primer (5′–3′)	Antisense Primer (5′–3′)
IL-6	CCTGAAGGAAAAGATCGCAGG	TACCACAATCATGGGAGCCG
PIgR	CAAGAAGGCAAAGAGGTCGT	TGTGATTCGGAGCGTGATTG
TNF-α	TAGCCCACGTTGTAGCCAA	GGTAACTGAGGTGGGAGAGG
GAPDH	GGCCTCCAAGGAGTAAGGTC	TCTCTTCCTCTCGTGCTCCT

2.11. Histopathological Examination of Liver and Intestine of Lamb

Tissue samples from the liver, duodenum, jejunum, ileum, and spleen collected in Section 2.9 were immersed in 4% paraformaldehyde solution for easy fixation. The tissue samples were embedded in paraffin blocks and cut into 3–5 μm thick sections. Hematoxylin–eosin (HE) staining was used for histopathological examination to observe the histomorphological changes of the liver and spleen. Lamb intestinal samples were sent to Borf Bio Ltd. for immunofluorescence sections for ZO-1 and IgA detection. Images were captured under identical conditions, and mean fluorescence intensity was quantified using ImageJ (version 1.53a) with fields per sample.

2.12. Fecal Microbial Analysis

Fecal samples collected at the end of the experimental period were used for 16S rRNA gene sequencing. Total microbial DNA was extracted from fecal samples using an appropriate extraction procedure. DNA concentration was quantified using a NanoDrop spectrophotometer (Thermo Fisher Scientific, Waltham, MA, USA), and DNA integrity was assessed by 1.2% agarose gel electrophoresis. The target variable region of the bacterial 16S rRNA gene was amplified using high-fidelity DNA polymerase, with sample-specific barcode sequences incorporated into the primers. PCR amplification conditions were kept consistent across samples, and negative controls were included to monitor potential contamination. The amplification products were purified using VAHTS DNA Clean Beads (Vazyme) (Vazyme, Nanjing, China) at a bead-to-sample volume ratio of 0.8:1. Purified amplicons were quantified using the Quant-iT PicoGreen dsDNA Assay Kit (Thermo Fisher Scientific, Waltham, MA, USA) and pooled according to the required sequencing depth. Sequencing libraries were prepared using the TruSeq Nano DNA LT Library Prep Kit (Illumina, San Diego, CA, USA) followed by library purification and quality assessment using agarose gel electrophoresis and an Agilent Bioanalyzer. Qualified libraries were subjected to high-throughput sequencing by Bena Biotech Ltd. (Wuhan, China).

The resulting sequencing data were used for downstream microbial community analysis. Operational taxonomic unit (OTU) composition was analyzed, and principal component analysis (PCA) was performed to visualize differences in microbial community composition among the CK, TKP-L, and TKP-R groups. Overall differences were evaluated using permutational multivariate analysis of variance (PERMANOVA) based on Bray–Curtis dissimilarities, with 9999 permutations. Pairwise comparisons were adjusted using the Benjamini–Hochberg procedure. Homogeneity of multivariate dispersion was assessed using a permutation-based test of distances to group centroids. Alpha diversity was assessed using the Chao1, Shannon, and Simpson indices. Differentially represented microbial taxa were further analyzed using linear discriminant analysis effect size (LEfSe), with an LDA score threshold of 2. Microbial functional profiles were predicted using PICRUSt2 and interpreted as exploratory predictions rather than direct measurements of microbial activity.

2.13. Detection of Changes in Jejunal Metabolites

Jejunal tissue samples collected at the end of the experimental period were subjected to untargeted metabolomic analysis by Bena Biotech Ltd. (Wuhan, China) using an ultra-performance liquid chromatography–tandem mass spectrometry (UPLC–MS/MS) system. The resulting metabolomic data were used to characterize differences in jejunal metabolite profiles among the CK, TKP-L, and TKP-R groups. Principal component analysis (PCA) was performed to explore overall variation in metabolite profiles. Differential metabolites were initially screened using variable importance in projection (VIP) scores greater than 1 and nominal p values less than 0.05. Multiple-testing correction was performed using the Benjamini–Hochberg procedure across metabolic features within each pairwise comparison. False discovery rate (FDR)-adjusted p values (q values) below 0.05 were considered statistically significant. Metabolite features meeting the initial screening criteria but not the FDR-adjusted significance threshold were considered exploratory candidates. Associations between fecal microbial taxa and jejunal metabolites were evaluated using Spearman's rank correlation analysis. Correlations with an absolute correlation coefficient ($|r|$) greater than 0.6 and an FDR-adjusted q value below 0.05 were retained for correlation network construction.

2.14. Correlation Analysis

Spearman's rank correlation analysis was used to assess associations between fecal microbial taxa and jejunal metabolites. p values from the correlation tests were adjusted for multiple comparisons using the Benjamini–Hochberg procedure. Correlations with an absolute Spearman correlation coefficient ($|r|$) > 0.6 and an FDR-adjusted p value (q value) < 0.05 were considered statistically significant and were retained for correlation network construction.

2.15. Statistical Analysis

Data are expressed as mean ± SEM. Normality and homogeneity of variance were assessed using the Shapiro–Wilk test and Levene's test, respectively. For normally distributed data with equal variances, one-way ANOVA followed by Tukey's post hoc test was used. When variances were unequal, Welch's ANOVA followed by the Games–Howell test was used. For non-normally distributed data, the Kruskal–Wallis test followed by Dunn's multiple-comparison test was used. Significance letters in figures were assigned based on these post hoc tests. For high-dimensional omics analyses, multiple-testing correction was performed using the Benjamini–Hochberg procedure where appropriate, and false discovery rate (FDR)-adjusted p values (q values) were reported. Overall differences in fecal microbial community composition and jejunal metabolite profiles were evaluated separately using permutational multivariate analysis of variance (PERMANOVA), with 9999 permutations. Homogeneity of multivariate dispersion was assessed independently to support the interpretation of PERMANOVA results. Principal component analysis (PCA) was used exclusively for exploratory visualization of overall data variation and was not considered evidence of statistically significant differences among groups. A permutation-based p value < 0.05 was considered statistically significant for PERMANOVA and dispersion tests. Given the relatively small sample size ($n = 7$ per group), the findings from 16S rRNA sequencing, LEfSe, untargeted metabolomics, and Spearman correlation analyses were interpreted as exploratory and require further validation.

For RT-qPCR analysis, individual-animal ΔCt values were calculated by subtracting the Ct value of the reference gene (GAPDH) from that of the target gene. Statistical comparisons among treatment groups were performed using ΔCt values rather than $2^{-\Delta\Delta Ct}$-transformed values. Relative gene expression was calculated using the $2^{-\Delta\Delta Ct}$ method and normalized

to the CK group for graphical presentation. Individual-animal variation was retained when calculating the descriptive statistics of relative expression.

3. Results

3.1. Network Pharmacology

Network pharmacology analysis identified 72 candidate targets for TKP-L and 41 candidate targets for TKP-R, while 5714 genes were associated with lamb growth- and immune-related diseases in the selected database. Venn diagram analysis identified 47 overlapping candidate targets for TKP-L and 27 for TKP-R (Figure 1A,B). Following PPI network construction using STRING with a confidence score threshold of 0.4, the resulting networks contained 38 nodes and 97 edges for TKP-L and 20 nodes and 33 edges for TKP-R (Figure 1C,D), respectively.

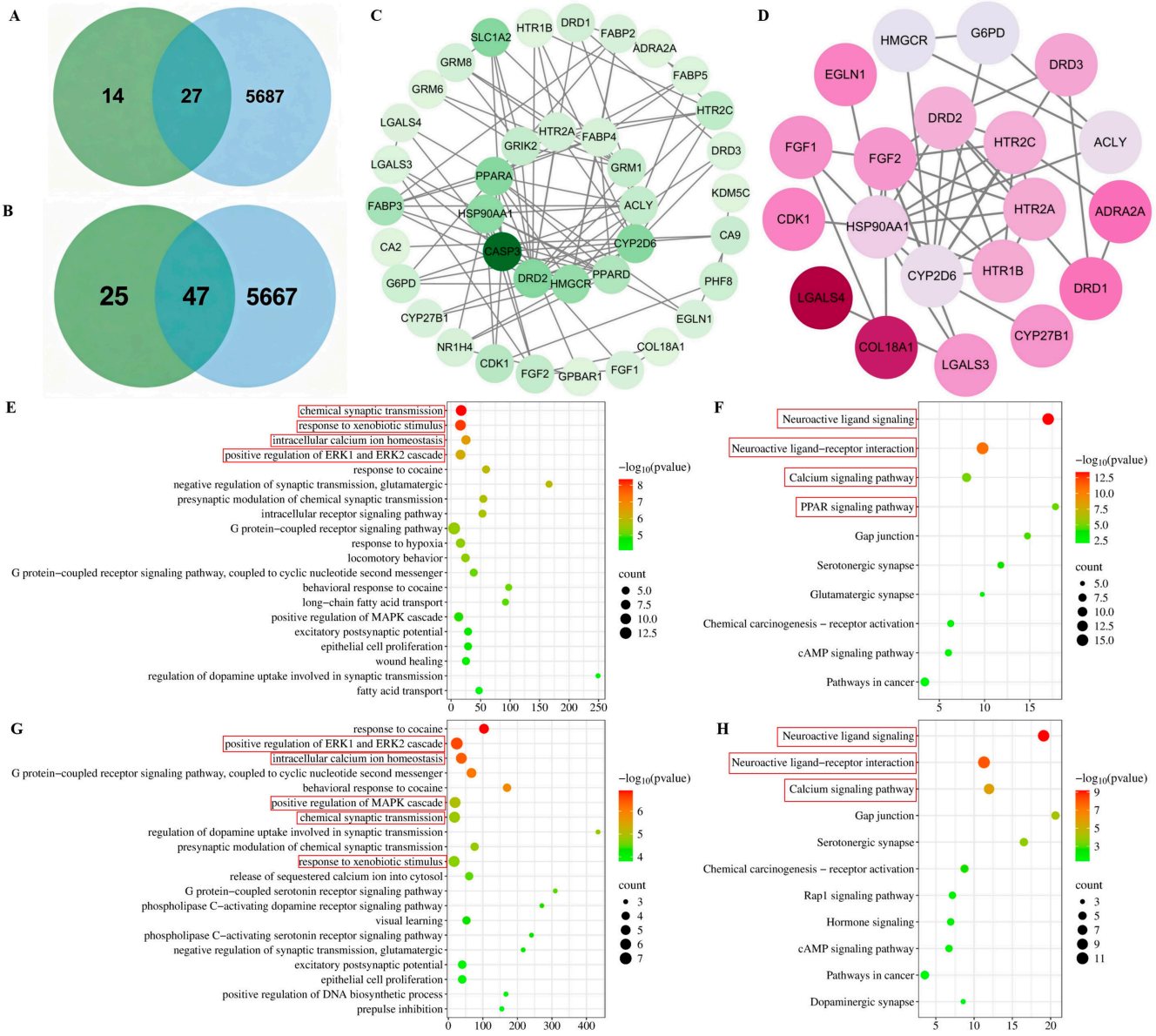


Figure 1. TKP-L, TKP-R, and lamb growth immune network pharmacology.

To clarify the biological function of TKP-L and TKP-R in the two groups of candidate targets and the potential mechanism of action, this study respectively focused on two groups of targets in the GO-BP function of enrichment and enrichment of KEGG pathway

analysis. The GO-BP enrichment results for the TKP-L group showed (Figure 1E) that its targets were mainly significantly enriched in biological processes such as chemical synaptic transmission, response to exogenous stimulation, intracellular calcium homeostasis, and positive regulation of the ERK1/2 cascade reaction, suggesting that TKP-L may play a biological role by regulating neural signal transmission and calcium signal homeostasis. The KEGG pathway enrichment results for TKP-L (Figure 1F) showed that the targets were mainly concentrated in the neural active ligand–receptor interaction, calcium signaling pathway, and PPAR signaling pathway, among which the neural active ligand–receptor interaction pathway was the most significantly enriched and was the predicted candidate pathway for TKP-L action. The GO-BP enrichment results for the TKP-R group (Figure 1G) showed that its targets were also enriched in neural signal regulation, stress response, and cell proliferation-related processes, which partially overlapped with TKP-L, and also showed a certain specificity, such as in the response to cocaine and the G protein-coupled receptor signaling pathway. It is suggested that TKP-R is more responsive to specific stress signals on the basis of neurotransmitter transmission and calcium signal regulation. The KEGG enrichment results predicted (Figure 1H) that neuroactive ligand–receptor interaction and the calcium signaling pathway were the most significantly enriched candidate pathways for TKP-L. These predictions require further validation in lamb tissues.

3.2. Effects of TKP-L and TKP-R on the Expression of Intestinal Immune-Related Gene mRNA in Lambs

As shown in Figure 2, after administration of TKP-L and TKP-R, the relative mRNA expression levels of selected intestinal immune-related genes were evaluated. Statistical comparisons were made using the ΔCt values of individual animals, while the relative gene expression was represented by $2^{-\Delta\Delta Ct}$ values. In the duodenum, no statistically significant differences were found in the mRNA expression levels of PIgR (Gamers–Hauer test), IL-6 (Tukey test), or TNF-α (Gamers–Hauer test) among the CK, TKP-L, and TKP-R groups. Although the expression level of PIgR in the TKP treatment group was numerically higher than that in the CK group, these differences did not reach the statistical significance level ($p > 0.05$). Similarly, there were numerical differences in the expression of PIgR mRNA in the jejunum among the three groups, but no statistically significant differences were observed (Kruskal–Wallis test). In contrast, the IL-6 mRNA expression in the jejunum showed significant inter-group differences overall (one-way ANOVA), and subsequent Tukey post hoc analysis revealed that the IL-6 expression in the TKP-L group was significantly higher than that in the TKP-R group (corrected p value = 0.004). However, the expression levels of IL-6 in the TKP-L group and TKP-R group did not show significant differences from the CK group. Overall, these results indicate that TKP-L and TKP-R are related to the numerical changes in the expression of intestinal immune-related genes. However, in this qPCR data set, only the statistically significant difference in IL-6 expression between the TKP-L group and TKP-R group was observed.

3.3. Effects of TKP-L and TKP-R on Liver and Spleen Histology

As shown in Figure 3: The results of HE staining of liver tissue showed that the hepatocytes in the CK group were loosely arranged, the structure of liver lobules was generally clear, and a small number of vacuole-like areas could be seen in the tissue. Compared with the CK group, the TKP-L group had a more regular hepatic lobule structure, tightly arranged hepatic cords, uniform cell morphology, and fewer vacuolar changes. The hepatic cords in the TKP-R group were arranged continuously, and the intrahepatic vascular structure was clearer and the integrity of hepatocytes better than in TKP-L group. Both of

them can improve liver tissue morphology, maintain the normal structure of liver cells, and reduce liver tissue damage in lambs.

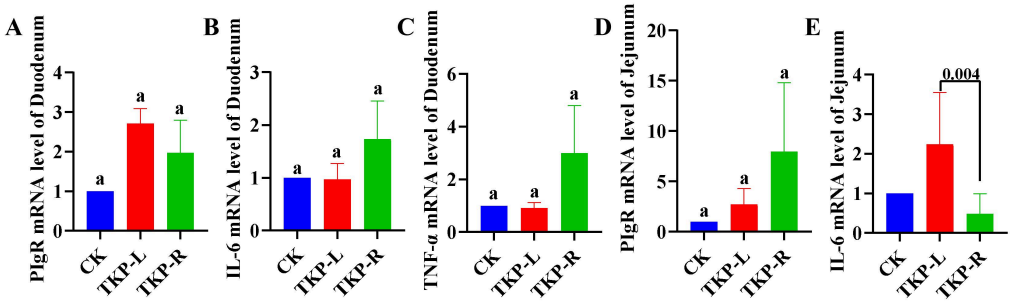


Figure 2. The relative mRNA expression of selected intestinal immune-related genes by TKP-L and TKP-R in lambs after 28 days of treatment: (**A**) duodenal PIgR; (**B**) duodenal IL-6; (**C**) duodenal TNF-α; (**D**) jejunal PIgR; (**E**) jejunal IL-6. CK represents the control group. The data are presented as mean ± standard error. Five samples were measured for the duodenum in each group, and seven samples were measured for the jejunum. The correlation analysis method is described in 2.15. Full [a] represents no significant difference between groups.

HE staining of spleen tissue showed that there were significant differences in the development of splenic white pulp (splenic lymphoid bodies) and the expansion of the splenic blood sinus in the red pulp of the spleen in each group. In the CK group, the number of splenic bodies was smaller, the volume was smaller, the boundary was distinguishable, the typical germinal center was not found, the red pulp splenic sinusoids were moderately dilated, and the distribution density of lymphocytes in the tissue was low. In the TKP-L group, the splenic bodies were more numerous, larger, and densely distributed, and the germinal center structure could be seen in some lymphoid follicles. The splenic sinusoid of the red pulp was slightly dilated with a high degree of lymphocyte enrichment. The white pulp was mature with significant characteristics of lymphocyte proliferation and activation. The splenic bodies of TKP-R were medium in number, uniform in size, and complete in outline. The splenic sinusoids of the red pulp were mildly dilated, the lymphocytes were evenly distributed, and the lymphoid tissue was moderately activated.

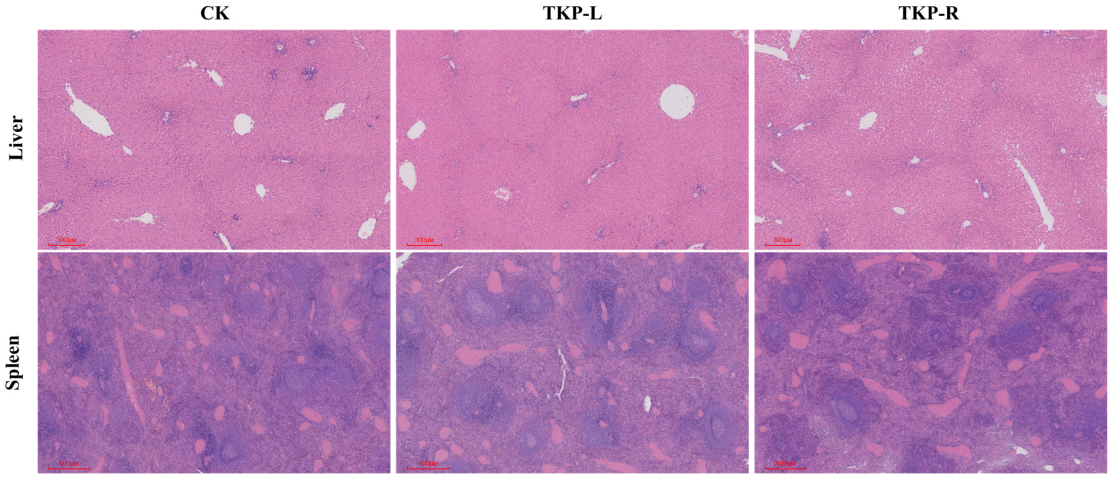


Figure 3. HE-stained sections of lamb liver and spleen.

3.4. Effect of TKP-L and TKP-R on Intestinal ZO-1 and IgA Expression

Immunofluorescence results of intestinal tissue showed that, compared with the CK control group, the ZO-1 fluorescence signal was visible, and the epithelial fluorescence

continuity and signal intensity in the TKP-R group were higher than in the TKP-L group, suggesting an improvement in a marker associated with intestinal barrier integrity. The intestinal mucosal IgA immunofluorescence intensity was numerically higher in the TKP-L group than in the TKP-R group, although no statistically significant difference was observed among the three groups. This trend suggests that leaf polysaccharides may have a potential effect on mucosal IgA-related immune responses; however, secreted sIgA was not directly measured in this study. These results indicate that polysaccharides from rubber roots and leaves have differential regulatory effects on intestinal barrier function. Polysaccharides from rubber roots focus on strengthening the physical barrier of the intestinal epithelium, while polysaccharides from leaves are more conducive to improving the intestinal mucosal immune function (Figure 4).

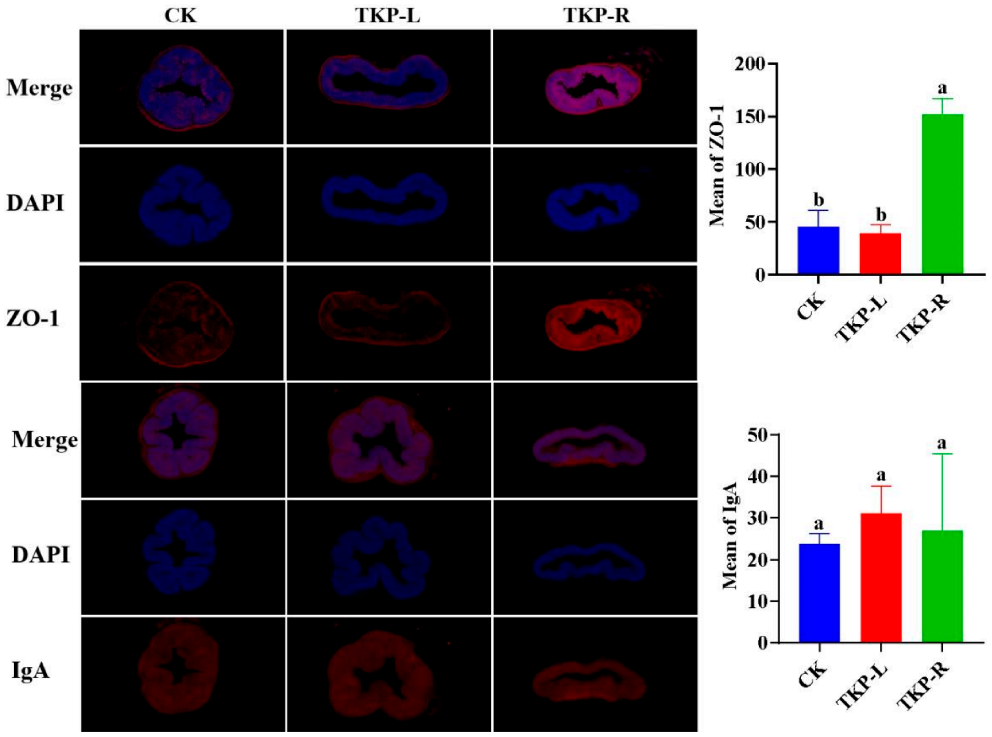


Figure 4. Fluorescence expression of ZO-1 and IgA in the intestine of lambs (Different letters represent differences between groups, and the same letters indicate no differences).

3.5. Analysis of Fecal 16S Flora

After analyzing the OTUs of fecal microorganisms of lambs in each group, the results showed (Figure 5A) that 38, 54, and 29 unique OTUs were obtained in the CK group, TKP-L group, and TKP-R group, respectively, and the number of common OTUs in the three groups was 38, suggesting that gavage of rubber weed polysaccharide could change the species composition of the fecal flora of lambs. Principal component analysis (PCA) was used to visualize differences in fecal microbial community composition among the CK, TKP-L, and TKP-R groups (Figure 5B). PC1 and PC2 explained 22.44% and 17.27% of the total variation, respectively. PERMANOVA based on Bray–Curtis dissimilarities revealed significant differences in overall microbial community composition among the three groups (pseudo-F = 3.942, R^2 = 0.305, p = 0.0001; 9999 permutations). Pairwise comparisons remained significant after Benjamini–Hochberg correction (CK vs. TKP-L, adjusted p = 0.0027; CK vs. TKP-R, adjusted p = 0.0015; TKP-L vs. TKP-R, adjusted p = 0.0076). The multivariate dispersion test did not detect a significant difference in within-group dispersion (p = 0.2883). These results provide statistical support for differences in

overall microbial community composition among the groups. Furthermore, the α diversity index was analyzed among groups (Figure 5C): the Chao1 index, Shannon index, and Simpson index showed no significant differences among the three groups ($p > 0.05$), and the rubber polysaccharide treatment did not significantly change the species richness and diversity of lamb fecal flora.

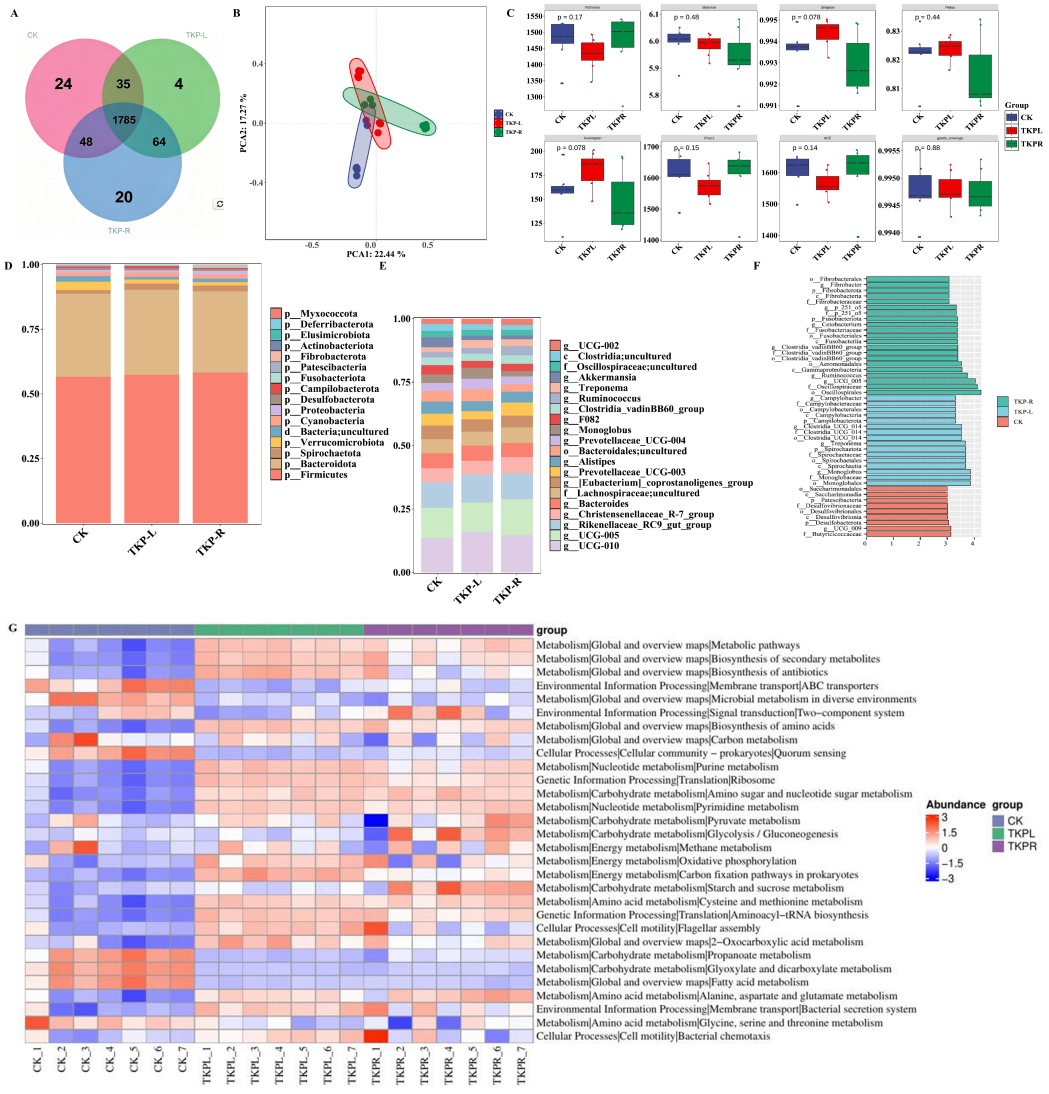


Figure 5. 16S-related changes in lamb feces (LEfSe analysis with an LDA score > 2). (**A**) VENN plot of otus among groups, (**B**) PCA plot between groups, (**C**) alpha diversity map, (**D**) Species composition at phylum level, (**E**) Species composition at the genus level, (**F**) LEfSe plot, (**G**) PICRUSt2 prediction map.

At the phylum level, the relative abundance of fecal microbial communities was analyzed for each group (Figure 5D): *Firmicutes* and *Bacteroidetes* were the dominant phyla in the fecal microbiota of the three groups, accounting for more than 90%. There was no significant difference in the relative abundance of *Firmicutes* and *Bacteroidetes* among the three groups ($p > 0.05$). In addition, there was no significant difference in the relative abundance of bacteria such as *Actinobacteriota* and *Proteobacteria* among the three groups. At the genus level, the top 20 bacterial genera in relative abundance were analyzed (Figure 5E): the dominant genera of fecal microbiota in the three groups mainly included *[Eubacterium]_coprostanoligenes_group*, *Oscillospiraceae_UCG-005*, and *Christensenellaceae_R-7_group*. Compared with

the CK group, the relative abundance of some bacterial genera in the TKP-L and TKP-R groups changed, but the difference between the two groups did not reach statistical significance ($p > 0.05$). Further LEfSe analysis was used to screen species that differed between groups (Figure 5F): Under the LDA score > 2 condition, the enriched species in the CK group were mainly *Eubacteriaceae*-related groups, and the enriched species in the TKP-L group were mainly *Oscillospiraceae*-related groups. The enriched species in TKP-R group were mainly *Ruminococcaceae*-related groups, suggesting that *Taraxacum kok-saghyz* Rodin polysaccharide treatment can induce the enrichment of specific groups in the fecal flora of lambs.

Prediction of the function of the lamb fecal microbial community based on PICRUSt2 was performed (Figure 5G): The functions of the three groups of microbiota were mainly concentrated in three pathways: Metabolism, Environmental Information Processing, and Cellular Processes. Compared with the CK group, the predicted relative abundances of pathways related to carbohydrate metabolism, energy metabolism, and amino acid metabolism showed increasing trends in the TKP-L and TKP-R groups, whereas pathways related to signal transduction showed a decreasing trend. These PICRUSt2-based predictions suggest potential differences in microbial functional profiles among groups; however, they do not directly demonstrate changes in microbial activity or host nutrient metabolism.

3.6. Changes in Jejunal Metabolites

In order to clarify the effects of TKP-L and TKP-R treatments on the jejunum tissue metabolome of lambs, in this study, the jejunum metabolites of the CK, TKP-L, and TKP-R groups were analyzed by non-targeted metabolomics technology. PCA was used to explore the overall variation in jejunal metabolite profiles among the CK, TKP-L, and TKP-R groups (Figure 6A). The first three principal components of the PCA model for all 21 biological samples explained 53.0% of the total variation. Although PCA revealed apparent variation in jejunal metabolite profiles among the three groups, PERMANOVA did not identify a statistically significant overall difference ($p = 0.2258$). Therefore, the observed metabolomic patterns and candidate differential metabolites were interpreted as exploratory findings rather than evidence of significant global metabolic alterations. The results of volcano plot analysis showed that, compared with the CK group, 197 differential metabolites were screened in the TKP-L group, including 92 up-regulated metabolites and 105 down-regulated metabolites (Figure 6B). A total of 154 differential metabolites were screened in the TKP-R group, of which 103 were up-regulated and 51 were down-regulated (Figure 6C), suggesting that both treatments had extensive effects on the expression of jejunal metabolites, and TKP-L induced more differential metabolites than TKP-R.

Further hierarchical clustering heat map analysis of differential metabolites showed that the expression patterns of differential metabolites in the two groups were significantly different from those in the CK group, and the expression patterns within the group were highly consistent (Figure 6D,E), suggesting that both treatments induced characteristic metabolic changes. Compared with the CK group, TKP-L treatment significantly changed the jejunum metabolic profile of lambs, which was manifested as the significant down-regulation of most inflammation-related lipid mediators (e.g., PGI2, Lipoxin B4) and harmful metabolites of flora (e.g., phenyl sulfate), accompanied by the up-regulation of a small number of anti-inflammatory and gut-protective alkaloids (e.g., Curine). These results suggest that TKP-L may play a role in maintaining intestinal health and protecting intestinal barrier function by inhibiting intestinal inflammation and improving the metabolic pattern of intestinal flora. Compared with the CK group, TKP-R treatment significantly increased the levels of anti-inflammatory polyunsaturated fatty acids and lipid mediators such as EPA, α-linolenic acid, and γ-linolenic acid, and the expression of NAD, 3-Ketosphinganine, and

other substances related to energy metabolism and inflammatory signals in the jejunum tissue of lambs. These results suggest that TKP-R may improve intestinal health by enhancing intestinal anti-inflammatory lipid metabolism and inhibiting oxidative stress and inflammatory signaling pathways.

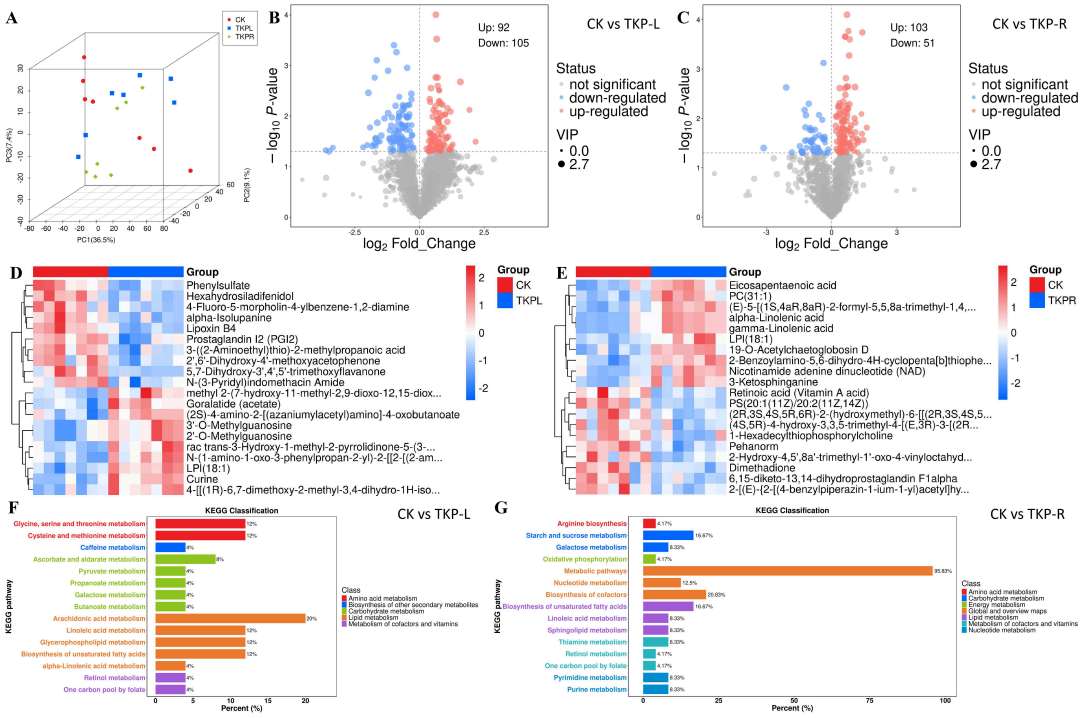


Figure 6. Changes in untargeted metabolites in the jejunum of lambs. (**A**) PCA plot of metabolite changes in each group; Volcano plots of differential metabolites in (**B**) CK vs. TKP-L group and (**C**) CK vs. TKP-R group; (**D**) hierarchical clustering heat map of differential metabolites in CK vs. TKP-L group and (**E**) CK vs. TKP-R group; KEGG pathway enrichment maps of (**F**) CK vs. TKP-L group and (**G**) CK vs. TKP-R group.

KEGG pathway enrichment analysis showed that the differential metabolites in the TKP-L group were mainly enriched in unsaturated fatty acid biosynthesis, glycine/serine/threonine metabolism, cysteine/methionine metabolism, and arachidonic acid metabolism (Figure 6F). The differential metabolites in the TKP-R group were mainly enriched in the overall metabolic pathway, arginine biosynthesis, starch and sucrose metabolism, and oxidative phosphorylation (Figure 6G), suggesting that the regulation patterns of jejunal metabolism were different between the two treatments: TKP-L mainly regulates amino acid and lipid metabolism pathways, while TKP-R affects energy metabolism and carbohydrate metabolism more generally.

3.7. Correlation Analysis

As shown in Figure 7A, Spearman correlation analysis showed that, after TKP-L intervention, *Prevotella* was significantly positively correlated with various immunomodulatory metabolites, LPI-18-1, and Curine, and was significantly negatively correlated with 3-methylglutaconic acid, a toxic byproduct of glycolysis. These results suggest that TKP-L may promote energy metabolism and reduce oxidative damage by enriching *Prevotella*. The abundance of mucin degradation bacterium *Monoglobus* was strongly negatively correlated with M3 receptor antagonist Hexahydrosiladifenidol, and TKP-L may have a potential inhibitory effect on *Monoglobus*. As shown in Figure 7B, *Cetobacterium* was significantly positively correlated with LPI-18-1 and eicosapentaenoic acid (EPA) after TKP-R intervention.

LPI-18-1, as an endogenous ligand of the GPR55 receptor, has a clear anti-inflammatory activity, and EPA is a potent anti-inflammatory n-3 polyunsaturated fatty acid. *Cetobacterium* mainly synthetes vitamin B12 and produces acetic acid by fermentation. Enrichment of *Cetobacterium* may regulate innate immunity by remodeling the intestinal microenvironment.

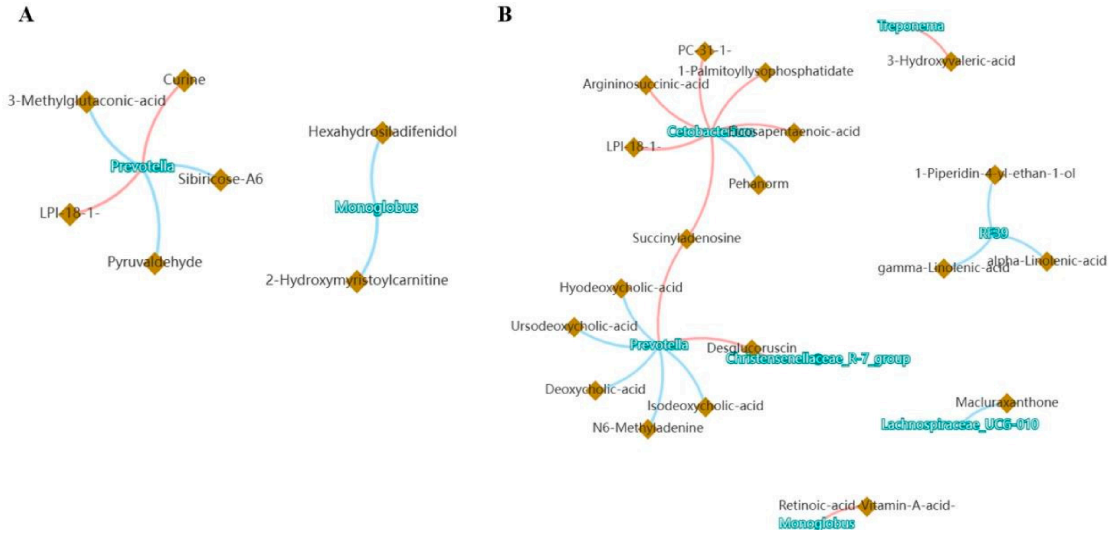


Figure 7. Correlation networks of microbiota and metabolites: (**A**) CK vs. TKP-L; (**B**) CK vs. TKP-R. Note: Dots in the figure indicate microorganisms, prisms indicate metabolites, larger shapes indicate higher abundance. Red lines indicate positive correlations, blue lines indicate negative correlations, and thicker lines indicate stronger correlations.

4. Discussion

The core hub proteins (HTR2A, DRD2, PPARA, and COL18A1) screened by PPI topology analysis of the network pharmacology in this study have been confirmed as key regulatory nodes of the gut–immune axis in multi-omics studies of polysaccharide intervention in ruminants in recent years. Among them, the 5-hydroxytryptamine receptor HTR2A mediates the secretion of 5-HT by intestinal chromaffin cells and regulates intestinal peristalsis and mucus secretion [12]. The DRD2 dopamine receptor can inhibit the excessive activation of macrophages and alleviate intestinal stress inflammation in weaned lambs [13]. These predictions guided the selection of measured parameters in the subsequent in vivo experiment. Specifically, the predicted involvement of immune-related pathways led us to measure PIgR, TNF-α, and IL-6 mRNA expression; the prediction of barrier-related targets prompted the assessment of ZO-1 and IgA by immunofluorescence; and the prediction of metabolic pathways informed the untargeted metabolomics analysis of jejunal metabolites. The measured results partially supported the predictions: TKP-L and TKP-R differentially regulated PIgR and cytokine expression, and the metabolomics results showed treatment-specific changes in amino acid and lipid metabolism. However, the predicted targets and pathways were not directly validated in lamb tissues, and the prediction was based on human databases and free monosaccharides rather than intact polysaccharides. Therefore, these results should be regarded as exploratory and hypothesis-generating, and further validation using targeted approaches (e.g., Western blot, immunohistochemistry, or receptor blocking experiments) is needed.

The intestinal mucosal defense system is composed of the physical tight junction barrier and the mucosal immune barrier mediated by secreted immunoglobulin A (sIgA), which together constitute the first line of defense against pathogen translocation in young lambs [14]. At the heart of the physical barrier is a network of tight junction proteins: ZO-1, as a skeleton protein, is expressed on the cytoplasmic side of the tight junction

of intestinal epithelial cells. By anchoring and combining the intracellular cytoskeletal microfilaments with the transmembrane proteins Occludin and Claudins, ZO-1 forms a complex network structure that closes the intercellular space, thus preventing pathogens and macromolecular substances from penetrating the intestinal epithelium through paracellular pathways [15]. In terms of the immune barrier, sIgA is synthesized by plasma cells in the intestinal lamina propria under the induction of cytokines such as IL-10 and TGF-β. After secretion, sigA is actively transported to the intestinal mucus layer through the polymerized immunoglobulin receptor (PIgR) expressed on the basal side of epithelial cells, and specifically binds to pathogens on the mucosal surface through immune exclusion. It promotes its excretion through intestinal peristalsis [16,17]. In this study, intestinal immunofluorescence quantitative results revealed the differential regulatory characteristics of the two types of rubber polysaccharides. The fluorescence continuity and signal intensity of ZO-1 in the TKP-R group were significantly higher than in TKP-L group, suggesting that TKP-R was more focused on physical barrier repair. The IgA immunofluorescence signal was stronger in the TKP-L group, suggesting that TKP-L may promote mucosal IgA-related immune responses. However, because secreted sIgA was not directly measured, this conclusion should be interpreted with caution. In summary, although both TKP-R and TKP-L can enhance the intestinal defense function of lambs, the focus of action is different: the former strengthens the physical tight junction, and the latter enhances mucosal humoral immunity, suggesting that the two can be applied differently for different intestinal health needs.

Intestinal qPCR results showed that both TKP-L and TKP-R could up-regulate the transcription level of PIgR, a key receptor mediating IgA transcytosis in the intestinal mucosa, but the two kinds of polysaccharides showed obvious tissue and target gene preferences. PIgR is a multimolecular immunoglobulin receptor synthesized and expressed by intestinal mucosal epithelial cells. Its core functions are to recognize and bind to dimeric sIgA secreted by plasma cells in the lamina propria, and to deliver sIgA from the lamina propria to the intestinal mucus layer through receptor-mediated transcellular transport, so as to complete the directed secretion of sIgA and mucosal immune exclusion [18,19]. Consistent with our findings, dietary yeast polysaccharides have been shown to improve immune function and intestinal barrier integrity in weaned lambs, including through increased IgG levels and enhanced expression of tight junction proteins [20]. Similarly, Alhagi camelorum Fisch polysaccharide supplementation in sheep lambs promoted intestinal secretory immunoglobulin A (sIgA) production and optimized local intestinal immune function by modulating cytokine expression [21]. In the present study, TKP-L increased PIgR mRNA and the IgA immunofluorescence signal in the duodenum, which is broadly consistent with the mucosal immunomodulatory effects reported for these polysaccharides. However, unlike studies that directly quantified sIgA, our study measured PIgR mRNA and IgA protein staining, and secreted sIgA was not directly determined. This distinction should be considered when comparing our results with those of previous studies.

Tnf-α has been reported to enhance PIgR expression in intestinal epithelial cells and may thus promote IgA transcytosis. In the present study, the moderate increase in Tnf-α and IL-6 induced by TKP may reflect immune activation; however, their potential pro-inflammatory effects should also be considered [22]. On the physiological basis that the immune system of young lambs is not yet mature and the basic immune activation signal is insufficient, the moderate and controllable increase in Tnf-α and IL-6 induced by TKP-L and TKP-R can be understood as an important activation signal to start the local intestinal immune defense network. This moderate inflammatory response can promote antigen presentation, immune cell recruitment, and maturation. It is fundamentally different from the persistent and pathological inflammatory storm caused by pathogenic infection.

Zhang isolated Turnips polysaccharide (BRP) from Xizang Turnips and found that it could significantly increase the secretion levels of IL-6, IL-10, Tnf-α, and immunoglobulin IgA in the serum of a cyclophosphamide-induced immunosuppression mice model [23]. It was further confirmed that BRP could regulate the expression of TLR4/Nf-κb signaling pathway-related genes, which provides a basis for dietary polysaccharides to enhance the body's defense ability by moderately activating the innate immune signal. The differences in tissue preference between TKP-L and TKP-R in cytokine induction and PIgR activation suggest that the two classes of polysaccharides may act through different pattern recognition receptors or downstream signal transduction pathways.

In this study, *Taraxacum kok-saghyz* Rodin polysaccharide treatment did not significantly alter the alpha diversity index of lamb fecal microbiota, which is consistent with the results of some plant polysaccharides. OTU composition analysis showed that unique OTUs appeared in the polysaccharide-treated group, indicating that *Taraxacum kok-saghyz* Rodin polysaccharide, as a prebiotic, can selectively promote the proliferation of specific bacterial communities and induce the reconstitution of bacterial community composition. This effect was further verified by PCA: The flora structure of the CK group and polysaccharide treatment group showed an obvious separation trend, indicating that plant polysaccharides had a general regulatory effect on the community structure of intestinal flora. At the phylum level, Firmicutes and Bacteroidetes were always the dominant phyla, which was consistent with the typical structure of the gut microbiota of ruminants. Firmicutes can secrete a variety of carbohydrate-active enzymes to decompose plant polysaccharides that are difficult for the host to digest and provide energy for the host. Bacteroidetes are mainly involved in the degradation of non-fiber carbohydrates [24,25]. In this study, there was no significant difference in the Firmicutes/Bacteroidetes ratio among the three groups, indicating that short-term polysaccharide intervention was not significant. The enrichment of Oscillospiraceae in the TKP-L group and Ruminococcaceae in the TKP-R group is consistent with previous reports that dietary polysaccharides selectively enrich specific functional bacterial taxa in ruminants. For example, Laminaria extract supplementation in Hu lambs enriched *Prevotella* and *Muribaculum*, while Jerusalem artichoke polysaccharide altered rumen microbiota composition at the genus level in fattening lambs [26]. Our finding that TKP treatment did not significantly alter α diversity but induced specific taxonomic shifts is also consistent with the observation that short-term polysaccharide intervention may not change overall diversity but can selectively promote certain functional groups. These comparisons support the prebiotic potential of TKP, although the specific taxa enriched differed among polysaccharide sources, likely reflecting differences in monosaccharide composition and molecular weight. Polysaccharides with different structures have different selective proliferation effects on intestinal flora. LEfSe analysis showed that Oscillospiraceae-related taxa were enriched in the TKP-L group, whereas Ruminococcaceae-related taxa were enriched in the TKP-R group, consistent with the results presented in Section 3.5. Other discriminative taxa identified by LEfSe are described according to their corresponding taxonomic assignments and group labels in Figure 5F. These findings suggest that TKP-L and TKP-R were associated with different patterns of fecal microbiota composition. The functional prediction results based on PICRUSt2 showed that *Taraxacum kok-saghyz* Rodin polysaccharide treatment could significantly affect the metabolic pathways of lamb fecal microbiota, such as the relative abundance of carbohydrate metabolism, nucleotide metabolism, and amino acid metabolism pathways. This result was consistent with the changes in the abundance of fiber-degrading bacteria such as Lachnospirillaceae and Ruminococcaceae. These predicted functional differences may reflect changes in the potential metabolic capacity of the fecal microbiota following TKP treatment; however, the PICRUSt2 predictions do not directly establish increased carbohydrate degradation, short-chain fatty

acid production, improved host nutrient utilization, or reduced production of potentially harmful nitrogen-containing metabolites. These possibilities require direct measurements and further functional validation.

The jejunum is the main site for the digestion and absorption of nutrients in ruminants, and its metabolic status directly affects the growth performance of the body. In this study, a variety of metabolites related to carbohydrate and protein digestion and absorption were significantly up-regulated in the TKP-L and TKP-R groups, such as metabolites involved in starch and cellulose decomposition, key intermediates of amino acid synthesis, etc. In this study, *Taraxacum kok-saghyz* Rodin polysaccharide treatment significantly altered several immune function-related pathways in the jejunum of lambs, such as amino acid metabolism, membrane transport, and cell motility. Among them, the activation of the amino acid metabolic pathway can promote the synthesis of immune-related proteins such as immunoglobulins and cytokines, and enhance the body's humoral and cellular immune functions [27]. The regulation of membrane transport-related pathways may be related to the up-regulation of intestinal tight junction protein expression, which can reduce the invasion of harmful substances and the risk of intestinal inflammatory response by improving the intestinal physical barrier function [28]. Previous studies have reported the immunomodulatory potential of *Taraxacum kok-saghyz* polysaccharides [10,11]. Liang et al. investigated TKP-L in a murine model of dysbiosis-associated mastitis, whereas the present study focused on intestinal immune-related responses in healthy lambs. Aersilan et al. examined growth performance, immune indices, rumen microbiota, and duodenal metabolites in lambs. In contrast, our study emphasized intestinal pIgR mRNA expression, ZO-1 and IgA immunofluorescence, fecal microbiota, and jejunal metabolites. Differences in experimental models, sampling sites, and measured outcomes may account for variations in the reported findings; however, overall jejunal metabolomic differences were not statistically significant, and microbiota–metabolite correlations do not establish causality. Thus, our findings complement previous research but require further functional and mechanistic validation. In this study, we found that there were significant differences in the regulatory effects of TKP-L and TKP-R on the jejunal metabolome of lambs. The regulation of energy metabolism-related pathways in the TKP-R group was more significant, focusing on the improvement of nutrient digestion and absorption and intestinal physical barrier function. However, the TKP-L group was more prominent in the regulation of amino acid metabolism and immune-related pathways, and more focused on providing raw material support for the growth and immune function of the body. This is partially consistent with a study on Jerusalem artichoke polysaccharide in fattening lambs, which reported that dietary polysaccharide supplementation altered ruminal metabolites involved in protein and fat metabolism. Laminaria extract was also reported to activate TCA cycle-centered metabolic profiles associated with immune modulation in Hu lambs. These comparisons suggest that dietary polysaccharides from different sources can differentially regulate host metabolism, and that the metabolic effects of TKP-L and TKP-R observed here are within the range of responses reported for other polysaccharides in ruminants.

Previous studies have reported the immunomodulatory potential of *Taraxacum kok-saghyz* polysaccharides [10,11]. Liang et al. [10] investigated TKP-L in a murine model of dysbiosis-associated mastitis, whereas the present study focused on intestinal immune-related responses in healthy lambs. Aersilan et al. [11] examined growth performance, immune indices, rumen microbiota, and duodenal metabolites in lambs; in contrast, our study emphasized intestinal pIgR mRNA expression, ZO-1 and IgA immunofluorescence, fecal microbiota, and jejunal metabolites. Differences in experimental models, sampling sites, and measured outcomes may account for variations in the reported findings; however, overall jejunal metabolomic differences were not statistically significant, and microbiota–

metabolite correlations do not establish causality. Thus, our findings complement previous research but require further functional and mechanistic validation.

5. Limitations

This study has several limitations: First, although seven biological samples per group were included in the microbiome and metabolomic analyses, the relatively small sample size ($n = 7$ per group) may have limited statistical power and reduced the precision of effect estimates, particularly in high-dimensional analyses such as LEfSe and Spearman correlation analysis. Therefore, findings from 16S rRNA sequencing, LEfSe, untargeted metabolomics, and Spearman correlation analyses should be considered exploratory and require validation in larger independent cohorts. Second, the network pharmacology analysis was based on human databases and free monosaccharides, and the predicted targets and pathways were not validated in lamb tissues; thus, these predictions can only generate hypotheses rather than establish mechanisms. Third, growth performance, feed conversion, nutrient absorption, intestinal barrier function, secreted sIgA, and the efficacy of TKP as a feed additive were not directly measured, so conclusions are restricted to the measured intestinal markers, fecal microbiota, and jejunal metabolites. Fourth, the exact pen area was not recorded, and temperature, relative humidity, and photoperiod were not continuously monitored; body weight and feed intake were not measured during the 7-day adaptation period. Fifth, the immunofluorescence and qPCR results reflect protein signals and mRNA levels, respectively, and do not directly demonstrate functional improvements in barrier integrity or IgA secretion. In addition, microbiota analysis was based on fecal samples, which may not fully represent the microbial composition of different intestinal segments, including the jejunum. Finally, although untargeted metabolomics identified candidate metabolite features with different abundance patterns, global PERMANOVA did not detect statistically significant differences in overall jejunal metabolomic profiles among the three groups ($p = 0.2258$). Therefore, these candidate features and KEGG pathway enrichment patterns should not be interpreted as conclusive evidence that TKP-L or TKP-R significantly altered jejunal metabolism. Claims regarding individual metabolites should be supported by FDR-adjusted q values, and their biological significance requires further confirmation through targeted metabolite quantification and functional validation. These limitations should be considered when interpreting the present findings.

6. Conclusions

Taraxacum kok-saghyz Rodin polysaccharide (TKP) has potential as a feed additive for ruminants; however, its efficacy was not evaluated in this study. In this study, TKP-L and TKP-R were associated with differential changes in selected intestinal immune markers, fecal microbiota composition, and jejunal metabolites in lambs. TKP-L was associated with higher PIgR mRNA expression and IgA immunofluorescence signaling in the duodenum, whereas TKP-R was associated with a higher ZO-1 signal. Both treatments enriched specific fecal taxa (TKP-L: *Oscillospiraceae*; TKP-R: *Ruminococcaceae*) without significantly altering α diversity and altered jejunal metabolites. However, secreted sIgA, intestinal barrier function, growth performance, nutrient utilization, and feed additive efficacy were not directly measured. The network pharmacology predictions were exploratory and were not validated in lamb tissues. These findings provide preliminary evidence and require further validation in larger cohorts and targeted mechanistic studies.

Author Contributions: X.Z.: writing—original draft preparation, methodology, data curation and formal analysis, validation; S.A.: review and editing, supervision; Y.Z.: review and editing, supervision, A.A.: investigation, supervision; Q.G.: investigation, supervision; A.K.: investigation, supervision,

J.C.: investigation, supervision; L.T.: investigation, supervision; T.T.: investigation, supervision; L.X.: review and editing, supervision; Z.M.: writing—review and editing, funding acquisition, project administration. All authors have read and agreed to the published version of the manuscript.

Funding: This work was supported by the following projects: the second round of support funds for the Xinjiang Uygur Autonomous Region Talent Development Fund in the 2025-Tianchi Talent Introduction Program; the Xinjiang Academy of Agricultural Sciences Science and Technology Innovation Stable Support Project (No. xjnkywdzc-2026003-01-7-5); the Tianshan Talent Training Program (2023TSYCLJ0010).

Institutional Review Board Statement: The animal study protocol was approved by the Animal Welfare and Ethics Committee of Xinjiang Agricultural University (2025020).

Informed Consent Statement: Not applicable. This study utilized publicly available databases (e.g., GeneCards, DisGeNET) that contain de-identified, aggregated data. No human participants were directly involved, and no individually identifiable information was accessed or analyzed.

Data Availability Statement: The data presented within the experimental framework are available on request from the first author. The 16S rRNA sequencing project has been registered with NCBI under BioProject accession PRJNA1545448 (https://www.ncbi.nlm.nih.gov/bioproject/1545448, accessed on 10 November 2026). All 21 BioSample records have been successfully processed, with accessions ranging from SAMN64268196 to SAMN64268216. The associated SRA data have been processed by NCBI and are currently scheduled for public release on 15 March 2029. The data presented within the experimental framework are available on request from the first author.

Conflicts of Interest: The authors declare no conflicts of interest.

References

1. Zhong, T.; Wang, Y.; Wang, X.; Freitas-de-Melo, A.; Li, H.; Zhan, S.; Wang, L.; Cao, J.; Dai, D.; Guo, J.; et al. Diarrhea in suckling lambs is associated with changes in gut microbiota, serum immunological and biochemical parameters in an intensive production system. *Front. Microbiol.* **2022**, *13*, 1020657. [CrossRef] [PubMed]
2. Shadi, A.; Mahdi, R. Antibiotic resistance and the alternatives to conventional antibiotics: The role of probiotics and microbiota in combating antimicrobial resistance. *Microbiol. Res.* **2023**, *267*, 127275. [CrossRef] [PubMed]
3. Bucataru, C.; Ciobanasu, C. Antimicrobial peptides: Opportunities and challenges in overcoming resistance. *Microbiol. Res.* **2024**, *286*, 127822. [CrossRef] [PubMed]
4. Bernabè, G.; Castagliuolo, I.; Porzionato, A.; Casarotto, G.; Monte, R.D.; Carpi, A.; Brun, P. Insoluble polysaccharides produced in plant cell cultures protect from Clostridioides difficile colitis. *Microbiol. Res.* **2024**, *286*, 127812. [CrossRef] [PubMed]
5. Qin, Y.; Xiong, L.; Li, M.; Liu, J.; Wu, H.; Qiu, H.; Mu, H.; Xu, X.; Sun, Q. Preparation of Bioactive Polysaccharide Nanoparticles with Enhanced Radical Scavenging Activity and Antimicrobial Activity. *J. Agric. Food Chem.* **2018**, *66*, 4373–4383. [CrossRef] [PubMed]
6. Wang, S.; Zhou, T.; Wang, X.; Zhao, J.; Wang, X. Bridging the gap: *Prevotella/Segatella's* impact on gut barrier function and advanced cultivation strategies to realize the uses in gut health. *Gut Microbes* **2026**, *18*, 2638001. [CrossRef] [PubMed]
7. Huang, Y.; Tang, J.; Cai, Z.; Zhou, K.; Chang, L.; Bai, Y.; Ma, Y. Prevotella Induces the Production of Th17 Cells in the Colon of Mice. *J. Immunol. Res.* **2020**, *1*, 960732. [CrossRef] [PubMed]
8. Guo, C.; Ma, D.; Zhang, C.; Wang, Y.; Ullah, F.; Wang, X.; Lee, Y.; Zhang, G. Dietary Jerusalem artichoke polysaccharide supplementation alters the growth performance, ruminal microbes and metabolites, muscle fatty acid and amino acid profiles in fattening lambs. *Anim. Nutr.* **2025**, *22*, 139–153. [CrossRef] [PubMed]
9. Bulat, K.; Kairat, U.; Gabit, B.; Elvina, B.; Khalit, G.M.; Alexey, V.C. Molecular Genetic Research and Genetic Engineering of *Taraxacum kok-saghyz* L.E. Rodin. *Plants* **2023**, *12*, 1621. [CrossRef] [PubMed]
10. Liang, Y.; Huang, P.; Li, J.; Manafu, Z.; Wang, R.; Chen, X.; Zhang, X.; Wu, Y.; Malajiang, X.; Yiming, A.; et al. The Protective Effects and Underlying Mechanisms of *Taraxacum kok-saghyz* Polysaccharides Against Intestinal Dysbiosis-Induced Mastitis Were Elucidated Using a Murine Model of the "Gut-Mammary" Axis. *Animals* **2026**, *16*, 751. [CrossRef] [PubMed]
11. Aersilan, A.; Manafu, Z.; Aosiman, G.; Zhang, X.; Tuxunjiang, Z.; Meng, Y.; Abula, S.; Wusiman, A. Mechanism underlying the regulation of gut microbiota-metabolite axis and growth/immune function in lambs by leaf-derived polysaccharides from *Taraxacum kok-saghyz*. *Front. Vet. Sci.* **2026**, *13*, 1799716. [CrossRef] [PubMed]
12. Shah, P.A.; Park, C.J.; Shaughnessy, M.P.; Cowles, R.A. Serotonin as a mitogen in the gastrointestinal tract: Revisiting a familiar molecule in a new role. *Cell. Mol. Gastroenterol. Hepatol.* **2021**, *12*, 1093–1104. [CrossRef] [PubMed]

13. Moore, S.C.; Vaz de Castro, P.A.S.; Yaqub, D.; Jose, P.A.; Armando, I. Anti-Inflammatory Effects of Peripheral Dopamine. *Int. J. Mol. Sci.* **2023**, *24*, 13816. [CrossRef] [PubMed]
14. Niu, X.; Yang, J.; Xing, Y.; Li, D. Plant Extracts to Enhancing Intestinal Barrier Function in Fattening lambs: A Review. *Anim. Biosci.* **2025**, *39*, 250496. [CrossRef] [PubMed]
15. Li, S.; Wang, C.; Zhang, L.; Chen, S.; Zhou, Y.; Yang, D.; Li, K.; Liu, Y.; Chi, S.; Wang, Y.; et al. Tight junction dysfunction and cytoskeletal remodeling in Hirschsprung-associated enterocolitis: A decade of mechanistic insights and therapeutic prospects (Review). *Mol. Med. Rep.* **2026**, *33*, 28. [CrossRef] [PubMed]
16. Johansen, F.E.; Kaetzel, C.S. Regulation of the polymeric immunoglobulin receptor and IgA transport: New advances in environmental factors that stimulate PIgR expression and its role in mucosal immunity. *Mucosal Immunol.* **2011**, *4*, 598–602. [CrossRef] [PubMed]
17. Okumura, R.; Takeda, K. The role of the mucosal barrier system in maintaining gut symbiosis to prevent intestinal inflammation. *Semin. Immunopathol.* **2024**, *47*, 2. [CrossRef] [PubMed]
18. Wei, H.; Wang, J.Y. Role of Polymeric Immunoglobulin Receptor in IgA and IgM Transcytosis. *Int. J. Mol. Sci.* **2021**, *22*, 2284. [CrossRef] [PubMed]
19. Wang, Y.; Xiao, J. Recent advances in the molecular understanding of immunoglobulin A. *FEBS J.* **2024**, *291*, 3597–3603. [CrossRef] [PubMed]
20. Li, X.; Meng, M.; Shi, H.; Zhou, S.; Ma, N.; Shen, X. Dietary supplementation of yeast polysaccharides enhance lamb growth performance by improving immune and intestinal barrier function and the abundance of cecal microbiota. *Int. J. Biol. Macromol.* **2025**, *309*, 142849. [CrossRef] [PubMed]
21. Manafu, Z.; Zhang, Z.; Malajiang, X.; Abula, S.; Guo, Q.; Wu, Y.; Wusiman, A.; Bake, B. Effects of Alhagi camelorum Fisch polysaccharide from different regions on growth performance and gastrointestinal microbiota of sheep lambs. *Front. Pharmacol.* **2024**, *15*, 1379394. [CrossRef] [PubMed]
22. Bruno, M.E.; Frantz, A.L.; Rogier, E.W.; Johansen, F.E.; Kaetzel, C.S. Regulation of the polymeric immunoglobulin receptor by the classical and alternative NF-κB pathways in intestinal epithelial cells. *Mucosal Immunol.* **2011**, *4*, 468–478. [CrossRef] [PubMed]
23. Zhang, Y.; Xu, Q.; Liu, Y.; Liu, Y.; Luo, J.; Liu, J.; Yu, S. *Brassica rapa* L. (Tibetan Turnip) polysaccharide improves the immune function and regulates intestinal microbiota in immunosuppressive mice. *J. Food Sci.* **2024**, *89*, 9816–9834. [CrossRef] [PubMed]
24. Zhu, N.; Yang, J.; Ji, L.; Liu, J.; Yang, Y.; Yuan, H. Metagenomic and metaproteomic analyses of a corn stover-adapted microbial consortium EMSD5 reveal its taxonomic and enzymatic basis for degrading lignocellulose. *Biotechnol. Biofuels* **2016**, *9*, 243. [CrossRef] [PubMed]
25. Cockburn, W.D.; Koropatkin, M.N. Polysaccharide Degradation by the Intestinal Microbiota and Its Influence on Human Health and Disease. *J. Mol. Biol.* **2016**, *428*, 3230–3252. [CrossRef] [PubMed]
26. Lin, M.; Li, J.; Chen, J.; Zhen, A.; Wajiha, W.; Li, S.; Li, X.; Zhang, S.; Tan, S.; Zhao, J.; et al. Laminaria extract reshapes the gut microbiota and TCA cycle-centered metabolic profiles associated with immune modulation in Hu lambs. *BMC Vet. Res.* **2026**, *22*, 605. [CrossRef] [PubMed]
27. Kelly, B.; Pearce, E.L. Amino Assets: How Amino Acids Support Immunity. *Cell Metab.* **2020**, *32*, 154–175. [CrossRef] [PubMed]
28. Arumugam, P.; Saha, K.; Nighot, P. Intestinal Epithelial Tight Junction Barrier Regulation by Novel Pathways. *Inflamm. Bowel Dis.* **2024**, *31*, 259–271. [CrossRef] [PubMed]

Disclaimer/Publisher's Note: The statements, opinions and data contained in all publications are solely those of the individual author(s) and contributor(s) and not of MDPI and/or the editor(s). MDPI and/or the editor(s) disclaim responsibility for any injury to people or property resulting from any ideas, methods, instructions or products referred to in the content.